Advanced Steel Construction – Vol. 17 No. 2 (2021) 127–135
DOI:10.18057/IJASC.2021.17.2.3

NUMERICAL STUDY AND DESIGN METHOD OF HIGH STRENGTH STEEL WELDED BOX COLUMNS

Yong-Jun Lin [1], Kai-Qi Liu [1], Tian-Ji Li [2] and Yi Zhou[*, 1]

[1] *School of Civil Engineering, Southwest Jiaotong University, 999 Xi'an road, Chengdu, Sichuan Province, China*
[2] *Shanghai Construction No.5 (Group) Co., Ltd., 1000 Cao yang road, Shanghai, China*
** (Corresponding author: E-mail: suzhouzhouyi@swjtu.edu.cn)*

ABSTRACT

In this paper, the buckling strength of HSS welded box columns was studied by means of numerical study, and the results were used to verify the applicability of provisions of buckling design in the current design codes and provide design recommendations. Fiber models were established taking into account for the effects of residual stress and geometric imperfection. Through the validation against the experimental results, these fiber models showed excellent capability of replicating the key test results, including buckling strengths and load-lateral deflection histories. Then a comprehensive parametric analysis was conducted to reveal the effects of steel grade and width to thickness ratio on column curves. The fiber model results were then compared with the design buckling strength factors from the current designs such as GB50017-2017, Eurocode 3 and ANSI/AISC 360-10. The comparison showed that the design codes could provide satisfactory accuracy in predicting buckling strength of HSS welded box columns by properly selecting columns curves. Furthermore, by updating the coefficients in the three current design codes, new column curves were proposed, which take the effects of yield strength and width-thickness ratio into consideration. The new column curves were proved to be able to predict the buckling strength with better accuracy and could facilitate the design of HSS welded box columns with different steel grades and width to thickness ratios.

ARTICLE HISTORY

Received: 19 April 2020
Revised: 29 December 2020
Accepted: 29 December 2020

KEYWORDS

High strength steel;
Welded box columns;
Global buckling;
Fiber model;
Column curve

1. Introduction

High strength steels (HSS) have yield strength more than 460MPa, which are prevailed in China and abroad. The GJ steel, as a typical high performance HSS, is created in China and increasingly applied in constructions [1-5]. In civil engineering, the commonly used steel grades for HSS columns include S460, S550, S690, S800 and S960 [6-10]. However, the applicability of current design codes in many countries is limited in the scope of normal strength steel (NSS) structures. For example, the Chinese code GB50017-2017 is not suitable for steel grades higher than S420 (420MPa) [11]. Though Eurocode 3 and ANSI/AISC 360-10 (2010) allow the use of HSS up to S700 (700 MPa) and A514 (690 MPa), the column curves in the design codes are on the basis of experiments and theoretical derivations of NSS with nominal yield strength from 235 MPa to 345 MPa [12-13].

In recent years, a series of axial compression experiments on columns made of HSS and GJ steel had been reported, where the main results include buckling capacity, typical failure mode, global and local buckling behaviors. It was concluded that the overall buckling behavior of HSS columns may be characterized differently from NSS columns due to different material properties and manufacturing processes. Furthermore, several researchers conducted experiments on residual stress and investigated its influence on overall buckling of HSS columns. The results indicated that the effects of initial geometric imperfections and residual stresses on buckling strength become less significant with increasing yield strength [14-20].

However, it was found that the existing researches are limited in conducting experiments on few specimens with one or several steel grades and sectional dimensions. Thus the column curves and design recommendations based on the experiments are unable to take material steel grade and sectional width to thickness ratio into consideration. As a result, the current design codes, such as Chinese code GB50017-2017, Eurocode 3 and American code ANSI/AISC 360-10 have not included these experimental results into provisions, making them not applicable to the buckling design of HSS columns [11-13].

This paper presented a numerical study in order to investigate the effect of material properties and sectional dimensions on buckling strength of HSS welded box columns. The buckling strengths of 1105 HSS welded box columns were obtained by means of fiber model and compared against the predictions of GB50017-2017, Eurocode 3 and ANSI/AISC 360-10. Based on the comparison, several recommendations were proposed for the design of HSS welded box columns subject to axial compression using the current codes. Furthermore, by updating the coefficients in the provisions, new column curves were proposed, which are described as functions of width to thickness ratio and nominal yield strength. The newly proposed column curves were proved to have better accuracy in predicting buckling strength of HSS welded box columns and could provide a unified design method for HSS welded box columns with different sectional dimensions and yield strength from 460MPa to 960MPa.

2. Recent experimental results

On the basis of the literature review on previous axial compression experiments, several databases were collected.

Wang et al. and Li et al. investigated the buckling performance of S460 and S690 welded box columns with different slenderness and width to thickness ratios and reported the corresponding load-deflection curves and load-strain curves [21-23].

Ban et al. tested a series of S960 welded box columns with the same sectional dimension but different slenderness to buckling and proposed design recommendations for buckling design using ANSI/AISC 360-10, Eurocode 3 and GB50017-2003 codes [17]. Furthermore, Ban et al. conducted experiments on welded box and I-shaped columns made of S460 steel, where the boundary condition of the specimens was not perfect pin-end support and the initial rotational stiffness of the hinges was measured [24].

Nie et al., Kang et al., Zhou and Xue et al. carried out experiments on GJ welded box columns, where the main results include buckling strengths, load-deflection curves and load-strain curves [1, 4, 5, 25]. According to the results, several supplements for ANSI/AISC 360-10, Eurocode 3 and GB50017-2003 codes were proposed.

Table 1 lists the dimensions and the buckling strengths of the specimens in the aforementioned experiments, where B is the sectional dimension, t is the plate thickness, L is the length, v_e is the initial loading eccentricity, v_0 is the initial bending, f_y is the yield strength of steel, E is the Elastic modules and P_u is the buckling strength.

Table 1
Specimens in collected database

HSS type	Reference	Specimen	B (mm)	t (mm)	L (mm)	v_e (mm)	v_0 (mm)	f_y (MPa)	E (GPa)	P_u (kN)
Conventional	Wang et al. [21]	B-8-80-1	110	11.40	3320	0.50	-3.50	506	208	1122
		B-8-80-2	112	11.49	3260	-0.9	1.50	506	208	1473
		B-12-55-1	156	11.43	3260	1.90	3.00	506	208	2591
		B-12-55-2	156	11.42	3260	-1.80	-2.00	506	208	2436
		B-18-38-1	220	11.46	3260	-0.60	3.00	506	208	3774
		B-18-38-2	221	11.46	3260	1.4	2.00	506	208	4010
	Li et al. [22-23]	B-30-2	236	16.10	2812	2.40	2.50	772	233	9751
		B-50-1	192	16.02	3610	0.10	-1.00	772	233	6444
		B-50-2	193	16.02	3612	-0.80	-1.50	772	233	7180
		B-70-1	141	16.07	3610	-0.80	-2.00	772	233	3528
		B-70-2	140	16.08	3609	0	-1.50	772	233	2897
	Ban et al. [17]	B1-960	143	13.99	1879	26.19	-0.31	973	208	3779
		B2-960	142	13.94	2880	-1.97	-1.16	973	208	4064
		B3-960	142	13.92	4382	3.45	-2.63	973	208	2193
GJ	Xue et al. [25]	460B50-150×12	155	12.46	3118	0	4.31	492	210	2508
		460B70-100×12	105	12.35	2828	0	3.05	492	210	1245
		550B110-75×12	77	12.51	3170	0	4.43	635	208	451
		550B30-100×12	101	12.60	1378	0	2.42	635	208	2057
		550B30-150×12	153	12.82	1987	0	0.95	635	208	4117
		550B50-100×12	102	12.60	2103	0	2.01	635	208	1900
		550B50-150×12	153	12.82	3118	0	0.82	635	208	3560
		550B70-100×12	102	12.60	2828	0	4.47	635	208	1177
		690B50-100×12	106	12.61	2103	0	0.78	727	211	2514
	Kang et al. [4]	B-120-12	120	12.23	3493	2.34	-1.22	546	209	1635
		B-168-12	168	12.45	4111	1.19	-2.44	546	209	2740
		B-264-12	264	12.21	3684	0.88	-3.12	546	209	5852
		B-175-25	176	21.53	5323	2.74	-0.12	473	209	3453
	Zhou [5]	B-200-25	201	25.42	5154	3.42	-1.37	473	208	4511
		B-225-25	226	25.33	4704	2.41	-1.75	473	208	6710
		B-250-25	251	25.32	3965	2.37	-2.25	473	208	8105
	Nie et al. [1]	B-120-45	121	12.54	3392	48.10	-2.58	557	208	862
		B-120-75	121	12.60	3391	79.40	1.16	557	208	643
		B-168-30	169	12.61	4009	28.60	-1.22	557	208	2004
		B-168-60	168	12.63	4009	58.80	1.51	557	208	1470
		B-216-45	217	12.57	4072	44.60	-1.14	557	208	2881
		B-216-75	217	12.55	4075	74.00	-3.61	557	208	2241
		B-264-30	264	12.59	3583	30.6	-0.96	557	208	4749
		B-264-60	265	12.63	3582	58.80	1.67	557	208	3900

3. Fiber model

3.1. Assumptions

According to the previous researches, the following assumptions are made for the fiber model [26-27]:

(1) A plane cross section remains plane after deformation.

(2) The deformation of structure consists with half-sinusoid.

(3) All members are assumed to be fully compact and adequately braced, thus local buckling and lateral torsional buckling are not considered.

(4) The influence of shear deformation is not considered.

3.2. Calculation method

The whole mid-span cross section is meshed into rectangular fibers for the preparation of numerical calculation, as shown in Fig. 1, where P is the load position of axial force and e_0 is the initial geometric imperfection to the mid-span section, which can be calculated by Eq. (1). Herein, each fiber is represented by its area and coordinate location corresponding to its centroid. The residual stresses are assigned directly to fibers as the initial stresses and the properties of the cross-section can be evaluated at each step of analysis [26].

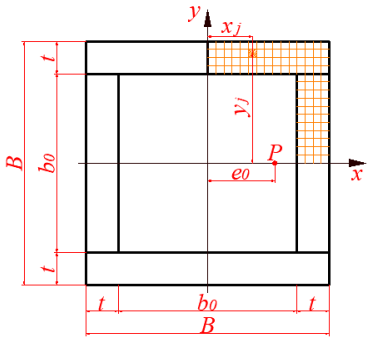

Fig. 1 Mesh fibers and sectional dimensions

$$e_0 = |v_e + v_0| \tag{1}$$

According to the assumption 2, the lateral deflection of axial compression member can be calculated by:

$$u_i = u_m \sin\frac{\pi}{L} z \tag{2}$$

where, u_i is the lateral displacement of section number i, u_m is the lateral displacement of mid-span section and z is the distance from the i section to the top end of the column.

The curvature of the mid-span section, ϕ_m, is:

$$\phi_m = u_m \frac{\pi^2}{L^2} \tag{3}$$

In the mid-span cross section, the coordinate of the fiber number j can be expressed as $(x_j,\ y_j)$, and the strain ε_j of the fiber is given by:

$$\varepsilon_j = \varepsilon_c + \phi_m x_j + \sigma_{rsj} / E \tag{4}$$

where, ε_c is the centroid strain of the section, σ_{rsj} is the residual stress of fiber number j and E is the elastic module.

Then the stress of the fiber number j can be calculated according to the constitutive relation:

$$\sigma_j = f(\varepsilon_j) \tag{5}$$

where the symbol '*f()*' represents the constitutive function of steel, as shown in Fig. 2 and defined by Eq. (6).

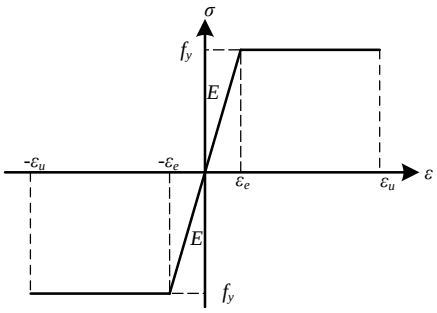

Fig. 2 Constitutive function of steel applied in fiber model

$$\sigma = \begin{cases} f_y & \varepsilon_e \le \varepsilon < \varepsilon_u \\ E\varepsilon & -\varepsilon_e \le \varepsilon < \varepsilon_e \\ -f_y & -\varepsilon_u \le \varepsilon < -\varepsilon_e \end{cases} \tag{6}$$

where, σ is the stress, ε_e is the elastic strain, ε_u is the ultimate strain.

Then, the internal axial force N_{in} and bending moment M_{in} can be calculated as:

$$M_{in} = \sum_{j=1}^{k} \sigma_j A_j x_j \tag{7}$$

$$N_{in} = \sum_{j=1}^{k} \sigma_j A_j \tag{8}$$

where k is the total number of fibers.

3.3. Residual stress

The residual stress has a strong influence on the buckling behavior of axial compression members, and the fiber models employing different residual models will result in different buckling strengths [17, 20, 28, 29]. A unified residual model suitable for HSS welded box columns of comprehensive steel grades and sectional dimensions was proposed by Ban et al., which could be further employed in the current numerical research [17, 20]. The shape of the unified model is presented in Fig.3 and the major parameters, such as width of tensile and compressive stress areas, magnitude of tensile stress and the self-balance conditions are listed in Tables 2-3.

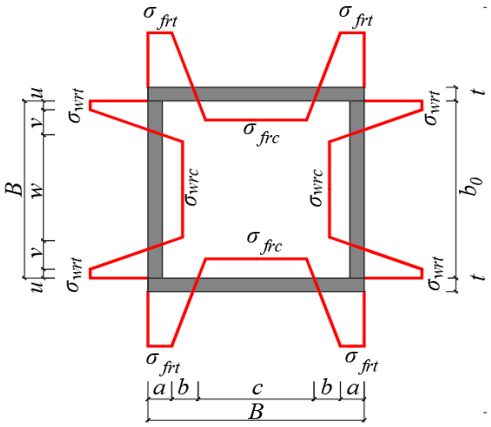

Fig. 3 Unified residual stress model

Table 2
Magnitude parameters of the unified residual stress model

σ_{frt}, σ_{wrt}		σ_{frc}, σ_{wrc}
460MPa $\le f_y \le$ 690MPa	460MPa	$\sigma_{rc} = -95 - \frac{1450}{h_0/t} - \frac{270}{t}$
$f_y \ge$ 690MPa	690MPa	$-f_y \le \sigma_{rc} \le -0.1 f_y$

Table 3
Location parameters of the unified residual stress model

a	u	b, c	v, w
$t + h_0/10$	t	$\iint_{A_f} \sigma_{rs} \cdot dA = 0$	$\iint_{A_w} \sigma_{rs} \cdot dA = 0$
		$2(a+b) + c = D$	$2(u+v) + w = b_0$

In Table 3, A_f is the area of flange, A_w is the area of web and σ_{rs} is the residual stress.

3.4. Equilibrium and calculation process

According to the assumption 4, the equilibrium of the mid-span section subject to axial compression and bending moment can be defined as:

$$M_{in} - N_{in}(e_0 + u_m) = 0 \tag{9}$$

where u_m is the deflection in the mid-span section oriented from bending moment.

Since the axial force N_{in} is coupled with the bending moment M_{in}, the mid-span deflection u_m and the mid-span curvature ϕ_m, an iterative method should be employed to find the solution of Eq. (9). Giving a specific mid-span curvature ϕ_m, the processes of iteration aiming to find the axial force N_{in}

corresponding to the ϕ_m and satisfying the equilibrium is presented in Fig. 4 [27].

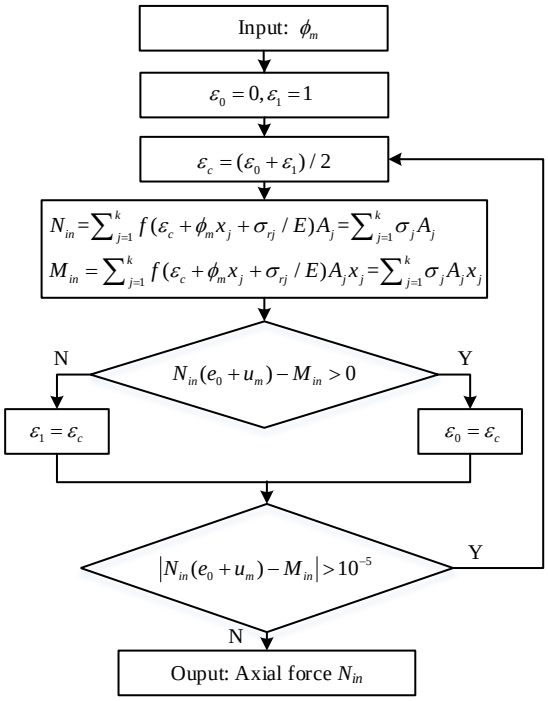

Fig. 4 Flowchart for iterative method

3.5. Calculation process

The calculation process includes the three steps:

a) Give a specific mid-span curvature ϕ_m ;

b) Calculate the deflection of the mid-span section u_m subject to the given ϕ_m according to Eq. (10);

c) Calculate axial load using the iterative strategy presented in Fig. 4.

The steps are repeated until the curvature of the mid-span section reaches a preset value and the whole load-deflection curve can be obtained. Then, the buckling strength can be set as the peak load. The specific processes are shown in Fig. 5.

$$u_m = \frac{L^2}{\pi^2}\phi_m \tag{10}$$

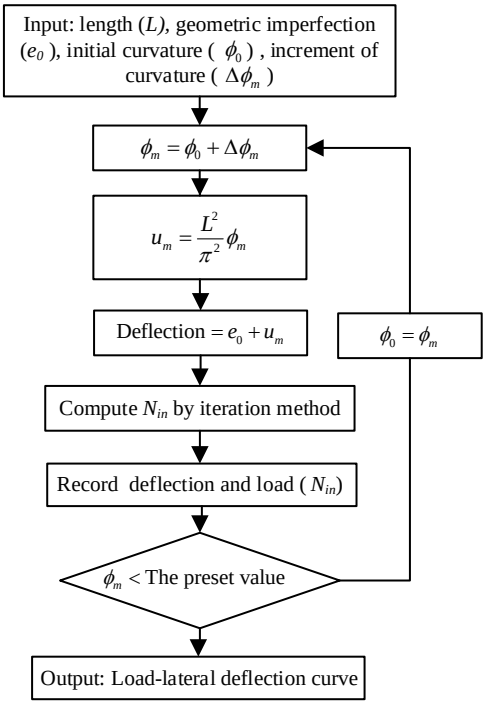

Fig. 5 Flowchart for calculation process

4. Model validation

To verify the accuracy, efficiency and versatility of the fiber model, HSS welded box columns under axial compression are analyzed and compared with the test data presented by several scholars. The buckling strengths of fiber models and the buckling strengths of test specimens are compared in Table 4. It can be seen that the buckling strength ratios range from 0.89 to 1.31 with an average of 1.05. Thus, the fiber models with unified residual stress model are able to capture the buckling strength of HSS welded box columns. The load-deflection curves obtained from the fiber models and test results are shown in Fig. 8. The comparison suggests that the numerical results are in good agreement with test results. Overall, it is concluded that the fiber models are capable of replicating the key test results.

Table 4
Comparison on buckling strength between test results and fiber models

Reference	Specimen	Test buckling strength (kN)	Fiber model buckling strength (kN)	Ratio
Wang et al. [21]	B-8-80-1	1122	987	1.14
	B-8-80-2	1473	1124	1.31
	B-12-55-1	2591	2220	1.17
	B-12-55-2	2436	2253	1.08
	B-18-38-1	3774	4178	0.90
	B-18-38-2	4010	4122	0.97
Li et al. [22-23]	B-30-2	9751	8680	1.12
	B-50-1	6444	5675	1.14
	B-50-2	7180	5551	1.29
	B-70-1	3528	3132	1.13
	B-70-2	2897	2825	1.03
Ban et al. [17]	B1-960	3779	3805	0.99
	B2-960	4064	3806	1.07
	B3-960	2193	2052	1.07
Xue et al. [25]	460B50-150×12	2508	2379	1.05
	460B70-100×12	1245	1109	1.12
	550B110-75×12	451	413	1.09
	550B30-100×12	2057	2323	0.89
	550B30-150×12	4117	4162	0.99
	550B50-100×12	1900	1794	1.06
	550B50-150×12	3560	3138	1.13
	550B70-100×12	1177	1178	1.00
	690B50-100×12	2514	2009	1.25
Kang et al. [4]	B-120-12	1635	1384	1.18
	B-168-12	2740	2595	1.06
	B-264-12	5852	6089	0.96
	B-175-25	3453	3269	1.06
Zhou [5]	B-200-25	4511	4550	0.99
	B-225-25	6710	6786	0.99
	B-250-25	8105	9427	0.86
Nie et al. [1]	B-120-45	862	826	1.04
	B-120-75	643	659	0.98
	B-168-30	2004	1970	1.02
	B-168-60	1470	1514	0.97
	B-216-45	2881	2966	0.97
	B-216-75	2241	2482	0.90
	B-264-30	4749	4917	0.97
	B-264-60	3900	4084	0.96

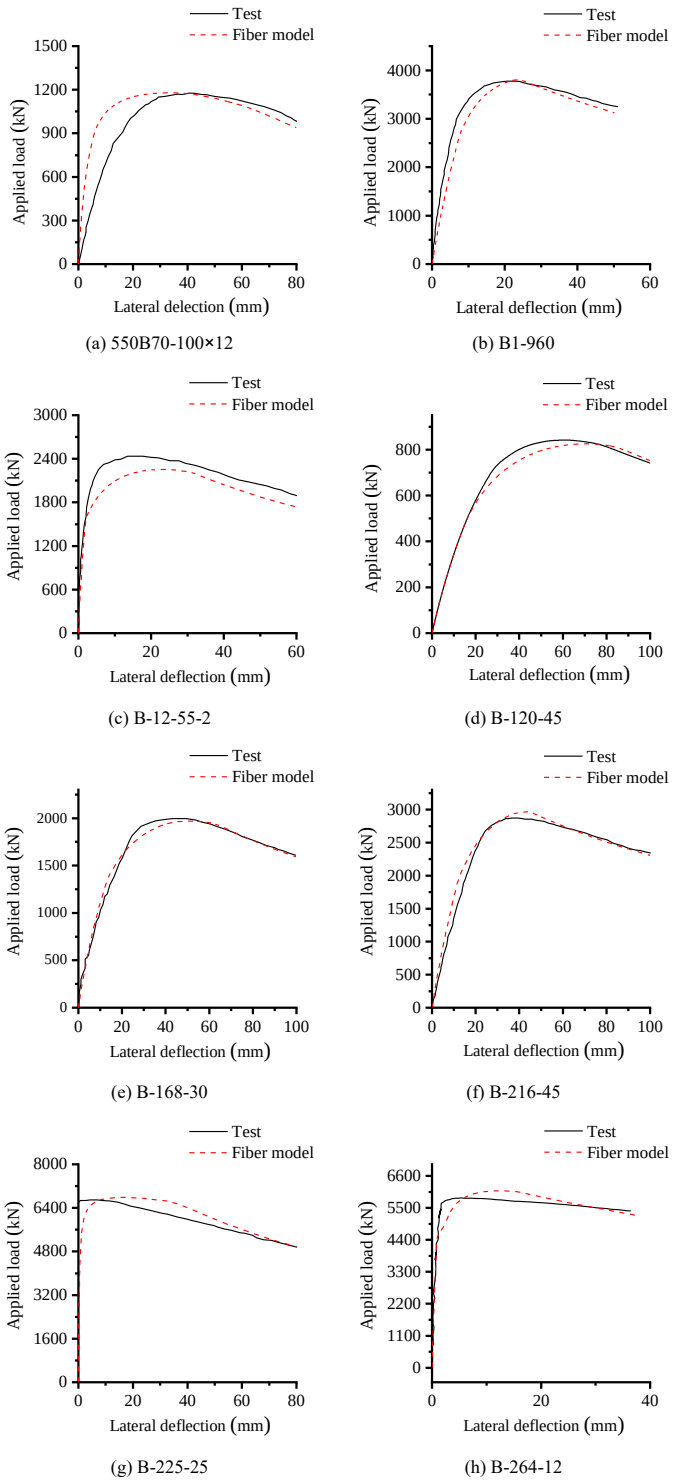

Fig. 6 Comparison on load-deflection curves between test results and fiber model results

5. Parametric studies and design recommendations

5.1. Parametric studies

Having validated the fiber models against the test results, a series of parametric studies are performed, focusing on steel grades and sectional width to thickness ratios. The sectional dimensions of specimens in the parametric study are listed in Table 5. For each sectional dimension, the slenderness varies from 10 to 130 with an interval of 10 corresponding to non-dimensional slenderness ranging from 0.15 to 3.0. And for each combination of sectional dimension and slenderness, the steel grades include S460, S550, S690, S800 and S960. The initial geometric imperfection is set as 1‰ of the specimen length covering unintentional load eccentricities and initial bending [11-13].

The buckling strength factors for each specimen are calculated according to the column curves in the design codes GB50017-2017, Eurocode 3 and ANSI/AISC 360-10. According to GB50017-2017, the curve c is used to design welded box columns with width to thickness ratios lower than 20 and curve the b is used to design welded box columns with width to thickness ratios higher than 20. According to Eurocode 3, the curve b is used to design welded box columns with width to thickness ratios higher than 30 and the curve c is used to design welded box columns with width-thickness ratios lower than 30. ANSI/AISC 360-10 code employs a single column curve to design all the welded box columns. The corresponding relations of sectional dimensions and design curves are listed in Table 5.

Table 5
Sectional dimensions of fiber models

Section	B (mm)	t (mm)	b_0/t	Design curve		
				GB50017-2017	Eurocode 3	ANSI/AISC 360-10
Sec-B1	77	13	3.92	Curve b	Curve c	Curve a
Sec-B2	101	13	5.77	Curve b	Curve c	Curve a
Sec-B3	201	25	6.04	Curve b	Curve c	Curve a
Sec-B4	140	16	6.75	Curve b	Curve c	Curve a
Sec-B5	120	12	8.00	Curve b	Curve c	Curve a
Sec-B6	251	25	8.04	Curve b	Curve c	Curve a
Sec-B7	192	16	10.00	Curve b	Curve c	Curve a
Sec-B8	155	12	10.92	Curve b	Curve c	Curve a
Sec-B9	168	12	12.00	Curve b	Curve c	Curve a
Sec-B10	250	11	20.73	Curve c	Curve c	Curve a
Sec-B11	220	10	20.00	Curve c	Curve c	Curve a
Sec-B12	270	12	20.50	Curve c	Curve c	Curve a
Sec-B13	380	14	25.14	Curve c	Curve c	Curve a
Sec-B14	360	12	28.00	Curve c	Curve c	Curve a
Sec-B15	390	12	30.50	Curve c	Curve b	Curve a
Sec-B16	350	10	33.00	Curve c	Curve b	Curve a
Sec-B17	211	6	33.17	Curve c	Curve b	Curve a

5.2. Applicability of current design codes

In GB 50017-2017 the buckling strength N_d of axial compression member is expressed as,

$$N_d = \varphi A f_y \tag{11}$$

where φ is the buckling strength factor.

When $\lambda_d \le 0.215$,

$$\varphi = 1 - a_1 \lambda_d^{\,2} \tag{12}$$

When $\lambda_d > 0.215$

$$\varphi = \frac{(a_2 + a_3\lambda_d + \lambda_d^{\,2}) - \sqrt{(a_2 + a_3\lambda_d + \lambda_d^{\,2})^2 - 4\lambda_d^{\,2}}}{2\lambda_d^{\,2}} \tag{13}$$

where λ_d is the non-dimensional slenderness, a_1, a_2 and a_3 are the imperfection factors.

The buckling strength of column in Eurocode 3 is defined as,

$$N_d = \varphi_e A f_y \tag{14}$$

where φ_e is the buckling strength factor.

When $\lambda_d \le 0.2$,

$$\varphi_e = 1 \tag{15}$$

When $\lambda_d > 0.2$,

$$\varphi_e = \frac{1}{0.5[1+a_E(\lambda_d-0.2)+\lambda_d{}^2]+\sqrt{\{0.5[1+a_E(\lambda_d-0.2)+\lambda_d{}^2]\}^2-\lambda_d{}^2}} \quad (16)$$

where, a_E is the imperfection factor.

In ANSI/AISC 360-10, the buckling strength of axial compression member is calculated by Eq. (17).

$$N_d = \varphi_c A f_y \quad (17)$$

where φ_c is the buckling strength factor.

When $\lambda_d \le 1.5$,

$$\varphi_c = a_{AN}{}^{\lambda_n{}^2} \quad (18)$$

When $\lambda_d > 1.5$

$$\varphi_c = 2.25\frac{a_{AN}{}^{2.25}}{\lambda_n{}^2} \quad (19)$$

where α_{AN} is the imperfection factor.

5.3. Comparison between fiber model and current design codes

Figs.7-9 show the buckling strength ratios of fiber models together with design results using column curves in the three design codes, where the S460, S690 and S960 specimens are selected to present the deviations. It is found that the deviations of the two methods are clear and increase with yield strength, which means the buckling strength of HSS welded box columns are generally underestimated by the current design codes. This fact is in agreement with the existing researches and can be explained by that the influence of initial imperfection and residual stress is less severe in the HSS structures compared with the NSS structures [30-31].

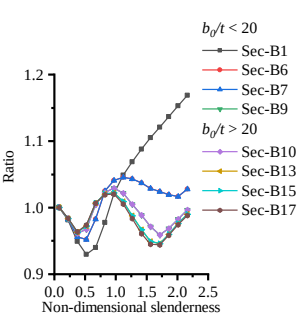

(a) GB50017-2017

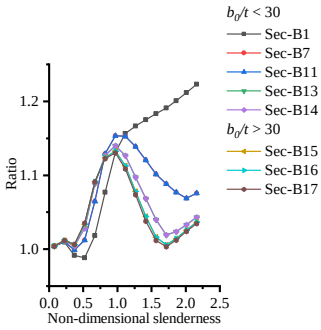

(b) Eurocode 3

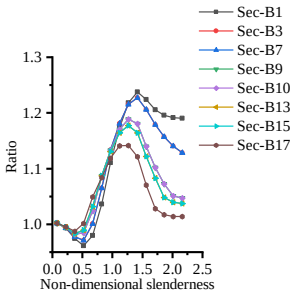

(c) ANSI/AISC 360-10

Fig. 7 Comparison of fiber model results and design results for S460 specimens

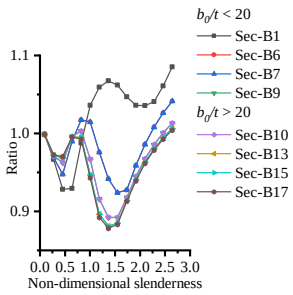

(a) GB50017-2017

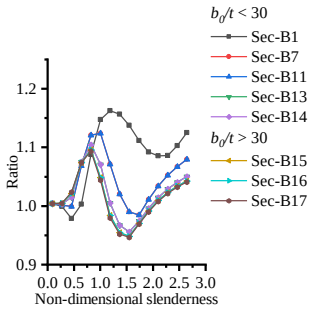

(b) Eurocode 3

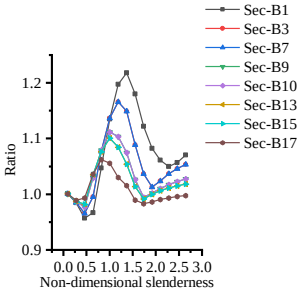

(c) ANSI/AISC 360-10

Fig. 8 Comparison of fiber model results and design results for S690 specimens

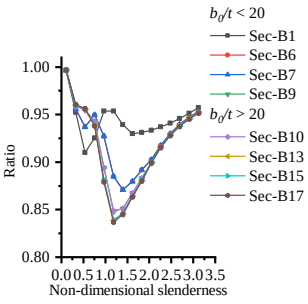

(a) GB50017-2017

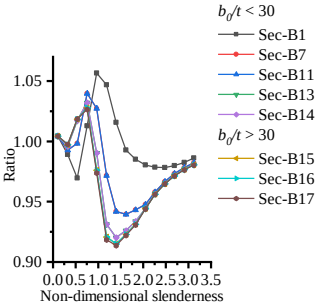

(b) Eurocode 3

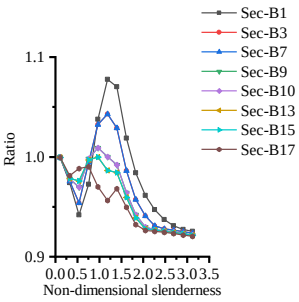

(c) ANSI/AISC 360-10

Fig. 9 Comparison of fiber model results and design results for S960 specimens

5.4. Recommendation on column curves

The errors between buckling strength factors using fiber models φ_{FM} and column curves in the three design codes φ_{DE} are calculated for all the parametric members by means of Eq. (20) and the mean errors of each steel grade are listed in Table 6.

$$\text{Error} = \frac{|\varphi_{FM}-\varphi_{DE}|}{\varphi_{FM}} \times 100\% \quad (20)$$

It is suggested that GB50017-20017 using curve b for all the steel grades while Eurocode 3 using curve b for steel grades lower than S800 and using c for steel grades higher than S800 could make predictions with satisfactory

accuracy to buckling strength of HSS welded box columns. Noting that if the column curve chosen according to the width to thickness ratio different from the column curve chosen according to the steel grade for one specimen, the buckling strength factor shall be the lower value obtained from the two column curves.

In the case of ANSI/AISC 360-10, it shows that most of the mean error values lie close to or lower than the recommended column curves in GB50017-2017 and Eurocode 3. And only the mean error of S460 specimens which is 7.55% lies between curve b and curve c in GB50017-2017 and slightly higher than curve c in Eurocode 3. Therefore, the column curve in ANSI/AISC 360-10 is also recommended to design HSS welded box columns.

Table 6
Average errors of buckling strength between numerical results and design curves

Steel grade	GB50017-2017			Eurocode 3			ANSI/AISC 360-10
	Curve b	Curve c	Recommendation	Curve b	Curve c	Recommendation	
S460	3.54%	9.05%	Curve b	3.16%	7.41%	Curve b	7.55%
S550	3.53%	11.84%	Curve b	3.79%	3.61%	Curve b	4.20%
S690	3.84%	10.52%	Curve b	3.88%	4.61%	Curve b	3.50%
S800	5.43%	12.80%	Curve b	5.87%	2.83%	Curve c	3.41%
S960	7.59%	14.32%	Curve b	8.07%	3.36%	Curve c	4.61%

5.5. Proposed column curve

In order to predict the buckling strength of HSS welded box columns with better accuracy for design, new column curves are proposed in this paper. The values of imperfection factors in the formula of column curves in Eurocode 3 (a_E), ANSI/AISC 360-10 (a_{AN}) and GB50017-2017 (a_2, a_3) are obtained using non-linear regression analysis on the buckling strength factors from parametric studies. The results are demonstrated in Figs. 10-11. It is found that the imperfection factors have a significant correlation with the width to thickness ratio and the nominal yield strength. Therefore, an empirical equation related to width to thickness ratio and nominal yield strength is suggested to calculate the imperfection factors of the column curves, as shown in Eq. (21), where a is the imperfection factor which is labeled as a_E in Eurocode 3, a_{AN} in ANSI/AISC 360-10 and a_3 in GB50017-2017 and f_y is the nominal yield strength (MPa).

$$a = (\alpha_1 + \alpha_2 \frac{b_0}{t}) \times (\alpha_3 + \alpha_4 \frac{f_y}{460}) \tag{21}$$

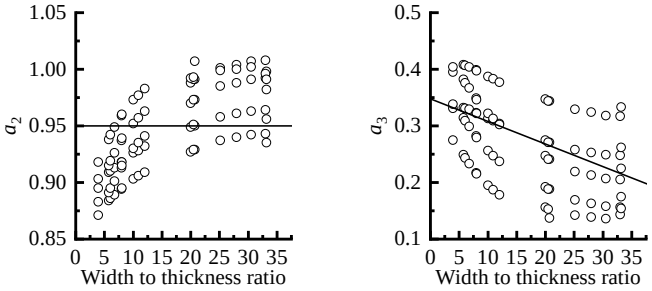

(a) a_2 of GB50017-2017 (b) a_3 of GB50017-2017

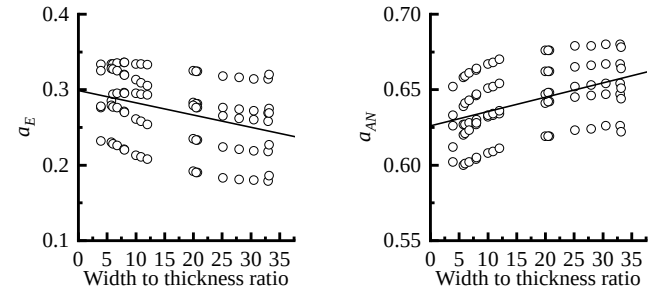

(c) a_E of Eurocode 3 (d) a_{AN} of ANSI/AISC 360-10

Fig. 10 The relation between imperfection factor and with to thickness ratio

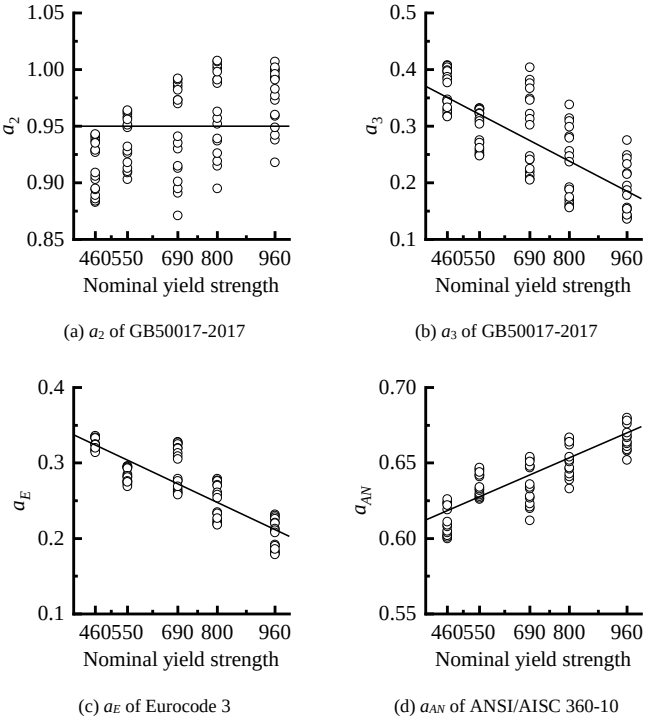

(a) a_2 of GB50017-2017 (b) a_3 of GB50017-2017

(c) a_E of Eurocode 3 (d) a_{AN} of ANSI/AISC 360-10

Fig. 11 The relation between imperfection factor and nominal yield strength

The values of regression coefficients α_1, α_2, α_3 and α_4 are listed in Table 7. For Eurocode 3 and ANSI/AISC 360-10, the imperfection factors a_E and a_{AN} can be calculated by Eq. (21). While for GB50017-2017, there are three coefficients to be determined, where the a_2 is settled as the average 0.95, the a_3 is determined by Eq. (21) and the a_1 is computed according to the continuity condition as shown in Eq. (22).

$$a_1 = \frac{2 \times 0.215^2 - (a_2 + 0.215a_3 + 0.215^2) + \sqrt{(a_2 + 0.215a_3 + 0.215^2)^2 - 4 \times 0.215^2}}{2 \times 0.215^4} \tag{22}$$

Table 7
Values of regression coefficients

Design code	Coefficient	Regression coefficients			
		α_1	α_2	α_3	α_4
GB50017-2017	a_3	2.590	−0.032	0.240	−0.071
Eurocode 3	a_E	1.780	−0.009	0.261	-6.27×10^{-2}
ANSI/AISC 360-10	a_{AN}	2.820	4.27×10^{-3}	0.198	0.0164

Fig. 12 depicts the comparison of mean errors of buckling strength factors using the recommended column curves and using the proposed column

curves for all the parametric specimens. It can be seen that the mean error using proposed column curves are smaller than the mean error using recommended column curves given in GB50017-2017, Eurocode 3 and ANSI/AISC 360-10. Fig. 13 depicts the buckling strength factors of selected specimens obtained from fiber models together with design results obtained from proposed column curves. It can be seen that the results obtained from the proposed curves are in good agreement with the results obtained from the fiber models. Overall, it is concluded that the proposed column curves are able to make predictions with better accuracy to buckling strength factors of HSS welded box columns with different width to thickness ratios and steel grades.

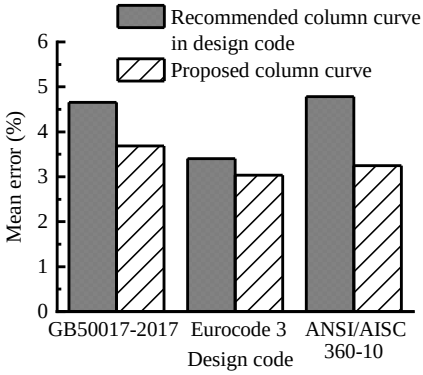

Fig. 12 Comparison of mean error between proposed column curves and design codes

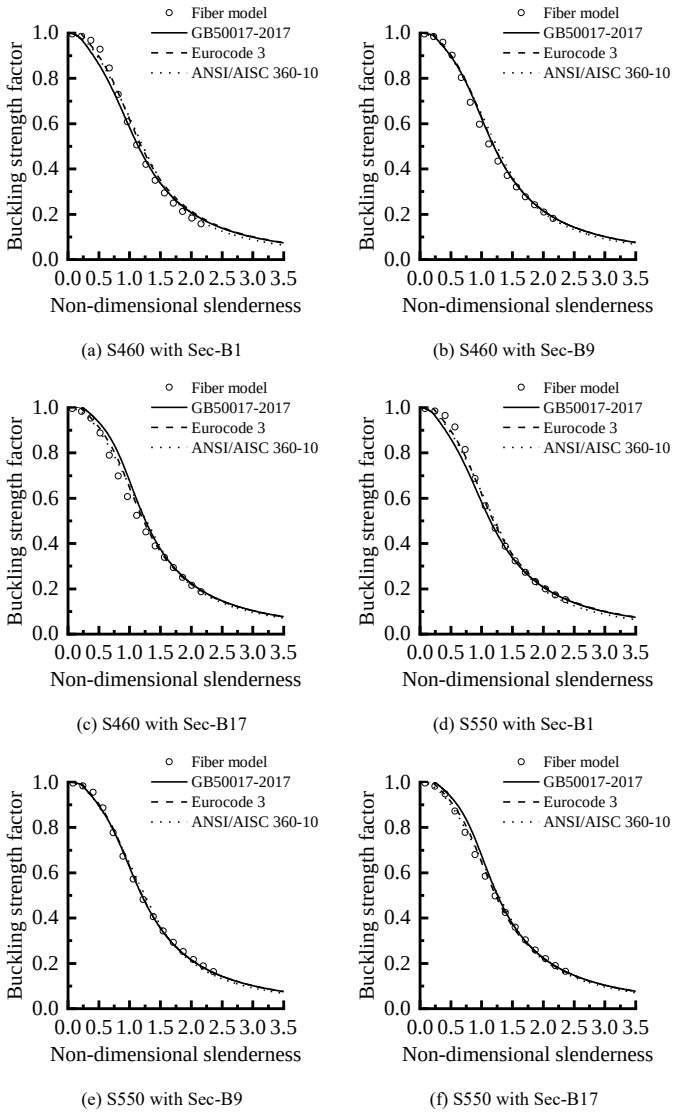

(a) S460 with Sec-B1 (b) S460 with Sec-B9

(c) S460 with Sec-B17 (d) S550 with Sec-B1

(e) S550 with Sec-B9 (f) S550 with Sec-B17

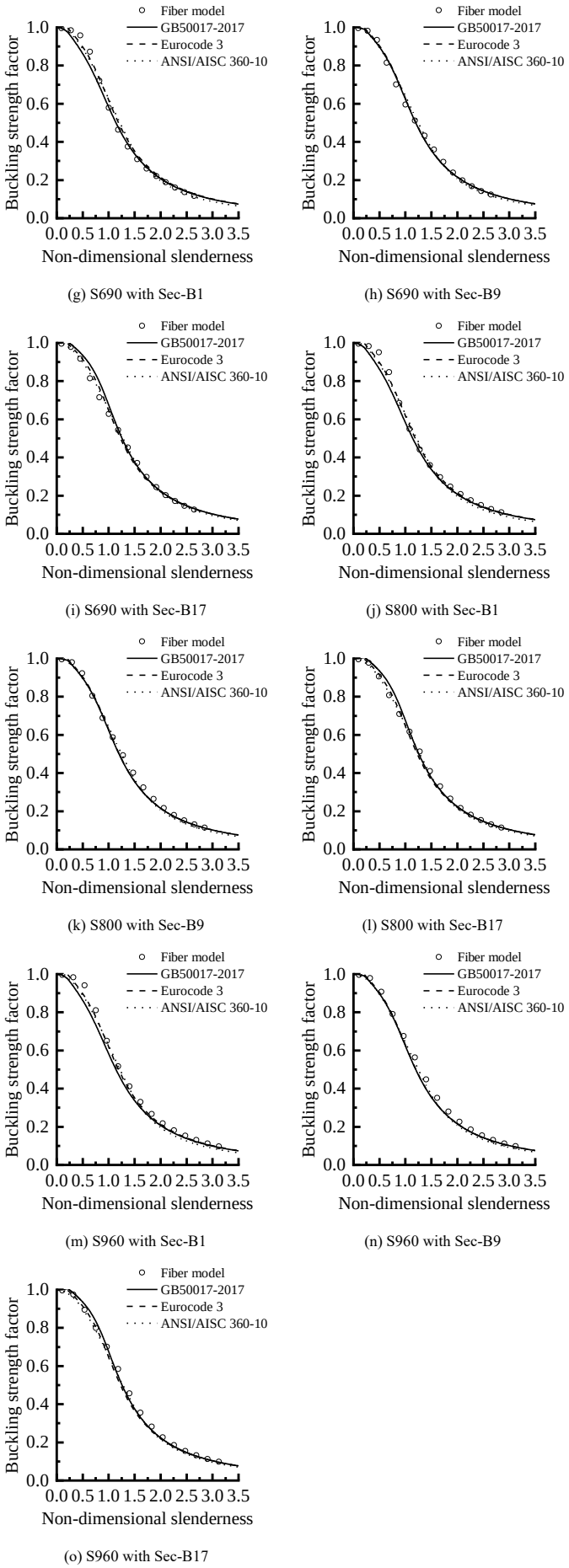

(g) S690 with Sec-B1 (h) S690 with Sec-B9

(i) S690 with Sec-B17 (j) S800 with Sec-B1

(k) S800 with Sec-B9 (l) S800 with Sec-B17

(m) S960 with Sec-B1 (n) S960 with Sec-B9

(o) S960 with Sec-B17

Fig. 13 Comparison of buckling strength factor between fiber model and proposed column curves

6. Conclusion

This paper conducted a numerical study on the buckling strength of HSS welded box columns with different steel grades under axial compression and to propose design recommendations for the current design codes. Fiber models employing unified residual stress model were established to replicate the experimental results of HSS welded box columns of different steel grades. Having the fiber models validated, parametric studies were carried out to investigate the effects of steel grade and width to thickness ratio on buckling strength of HSS welded box steel columns. The results are used to assess the applicability of current design codes including GB50017-2017, Eurocode 3 and ANSI/AISC 360-16 on buckling design of HSS welded box columns with different steel grades and sectional dimensions. The following conclusions have been made:

a)The fiber model employing unified residual stress model could accurately replicate the key test results.

b)The buckling strength factors of HSS welded box columns of different steel grades subject to axial compression from design codes GB50017-2017, Eurocode 3 and ANSI/AISC 360-10 are inconsistent with the buckling strength factors from fiber models. The average deviation of the whole parametric specimens is 8.37%, 4.7% and 4.6%, respectively.

c)In determination of buckling strength factor of HSS welded box columns subject to axial compression, the design rules in GB50017-2017 using curve b, the design rules in Eurocode 3 using curve b for steel grades lower than S800, the design rules in Eurocode 3 using curve c for steel grades higher than S800 and the design rules in ANSI/AISC 360-10 using single curve are recommended.

d) By updating the coefficients in the current design codes, new column curves are proposed, which takes the effects of material steel grade and sectional width to thickness ratio into consideration. The newly proposed column curves provide a unified method for the design of HSS welded box columns.

Acknowledgments

The authors are grateful to the financial support of the Natural Science Foundation of China (No.51608453).

References

[1] Nie S.D., Kang S.B., Shen L., Yang B., “Experimental and numerical study on global buckling of Q460GJ steel box columns under eccentric compression”, Engineering Structures, 142, 211-222, 2017.

[2] Y B., Nie S.D., Xiong G., Hu Y., Bai J.B., Zhang W.F., Dai G.X., “Residual stresses in welded I-shaped sections fabricated from Q460GJ structural steel plates”, Journal of Constructional Steel Research, 122, 261-273, 2016.

[3] Yang B., Xiong G., Ding K., Nie S.D,, Zhang W., Hu Y., and Dai G., “Experimental and numerical studies on lateral torsional buckling of welded Q460GJ structural steel beams” , Engineering Structures, 126, 1-14, 2016.

[4] Kang S.B., Yang B., Zhou X., Nie S.D., “Global buckling behaviour of welded Q460GJ steel box columns under axial compression”, Journal of Constructional Steel Research, 140, 153-162, 2018.

[5] Zhou X, “Global Buckling Behaviour of Welded Q460GJ Steel Box Columns under Axial Compression”, Licentiate Thesis, Chongqing University, Chongqing, China, 2017

[6] Ban H.Y., Shi G., Shi Y.J., “Overall buckling behavior and design method for axially compressed welded I-sectional columns constructed with different grades of high-strength steels”, CHINA CIVIL ENGINEERING JOURNAL, Vol. 47 No.11, 2014.

[7] Cao X., Gu L., Kong Z., Zhao G., Wang M., Kim S., Jia D. and Ma C., “Local buckling of 800 MPa high strength steel welded T-section columns under axial compression”, Engineering Structures, 194, 196-206, 2019.

[8] Yang H., Yang X.Q., Varma A.H. and Zhu Y., “Strain-Rate Effect and Constitutive Models for Q550 High-Strength Structural Steel”, Journal of Materials Engineering and Performance, 28, 6626-6637, 2019.

[9] Mursi M., Uy B. “Behaviour and design of fabricated high strength steel columns subjected to biaxial bending. Part 1: Experiments”, Advanced Steel Construction, 2(4), 286–313, 2006.

[10] Mursi M., Uy B., “Behaviour and design of fabricated high strength steel columns subjected to biaxial bending. Part 2: Analysis and design codes”, Advanced Steel Construction, 2(4), 314–354, 2006.

[11] GB 50017–2017 Code for design of steel structures, China Architecture &Building Press, Beijing, China, 2018.

[12] BSI, Eurocode 3, Design of Steel Structures—Part 1-1: General Rules and Rules for Buildings, British Standards Institution, London, 2003.

[13] ANSI/AISC360-10, Specification for Structural Steel Buildings, American Institute of Steel Construction, Chicago, Illinois, 2010.

[14] Li D., Paradowska A., Uy B., Wang J. and Khan M., “Residual stresses of box and I-shaped columns fabricated from S960 ultra-high-strength steel”, Journal of Constructional Steel Research, 166, 105904, 2020.

[15] Hussain A., Liu Y.P. and Chan S.L., “Finite Element Modeling and Design of Single Angle Member Under Bi-axial Bending”. Structures, 16, 373-389, 2018.

[16] Hussain A., Du Z.L., Liu Y.P. and Chan S.L., Stability design of single angle member using effective stress-strain method. Structures, 20, 298-308, 2019.

[17] Ban H.Y., Shi G., and Shi Y, “Experimental study on residual stress in 960MPa high strength steel welded box sections and unified model”, CHINA CIVIL ENGINEERING JOURNAL, 46(11), 63-69, 2013.

[18] Nie S.D., Zhu Q., Yang B., Li P.C., “Investigation of residual stresses in Q460GJ steel plates from medium-walled box sections” Journal of Constructional Steel Research, 148, 728-740, 2018.

[19] Li T.J., Li G.Q., Wang Y.B., “Residual stress tests of welded Q690 high-strength steel box- and H-sections” , Journal of Constructional Steel Research, 115, 283-289, 2015.

[20] Somodi B., Kövesdi B., “Residual stress measurements on welded square box sections using steel grades of S235–S960”, Thin-Walled Structures, 123, 142-154, 2018.

[21] Wang Y.B., Li G.Q., Chen S.W., Sun F.F., “Experimental and numerical study on the behavior of axially compressed high strength steel box-columns”, Engineering Structures, 58, 79-91, 2014.

[22] Li T.J., Li G.Q., Chan S.L., Wang Y.B., “Behavior of Q690 high-strength steel columns: Part 1: Experimental investigation”, Journal of Constructional Steel Research, 123, 18-30, 2016.

[23] Li T.J., Liu S.W., Li G.Q., Chan S.L., Wang Y.B., “Behavior of Q690 high-strength steel columns: Part 2: Parametric study and design recommendations”, Journal of Constructional Steel Research,122, 379-394, 2016.

[24] Ban H.Y., Shi G., Shi Y.J., Wang Y.Q., “Overall buckling behavior of 460 MPa high strength steel columns: Experimental investigation and design method”, Journal of Constructional Steel Research, 74, 140-150,2012.

[25] Xue, J.Y, “Experimental Research on the Overall Buckling Behavior of High Strength Steel Members under Compression”, Licentiate Thesis, Southeast University, NanJing. China., 2014

[26] Cuong N.H., Kim S.E., Oh J.R., “Nonlinear analysis of space steel frames using fiber plastic hinge concept”, Engineering Structures, 29, 649-657, 2007.

[27] Li, T., Liu, S. and Chan, S. “Cross-sectional analysis of arbitrary sections allowing for residual stresses”, Steel and composite structures, 18(4), 985-1000, 2015.

[28] Ban H.Y., Shi G., Shi Y.J., Wang Y.Q., “Residual stress of 460 MPa high strength steel welded box section: Experimental investigation and modeling”, 64, 73-82, 2013.

[29] Khan M., Paradowska A., Uy B., Mashiri F., Tao Z., “Residual stresses in high strength steel welded box sections”, 116, 55-64, 2016.

[30] Fang H. and Chan T., “Buckling resistance of welded high-strength-steel box-section members under combined compression and bending”, Journal of Constructional Steel Research, 162 105711, 2019.

[31] Han H., Chan T.M., “Buckling resistance of welded high-strength-steel box-section members under combined compression and bending”, Journal of Constructional Steel Research, 162, 150711, 2019.